Hydrobiologia **469:** 165–178, 2002.
S.A. Ostroumov, S.C. McCutcheon & C.E.W. Steinberg (eds), Ecological Processes and Ecosystems.

Microbial community analysis by FISH for mathematical modelling of selective enrichment of gel-entrapped nitrifiers obtained from domestic wastewater

Christian Vogelsang[1], Andreas Schramm[2], Cristian Picioreanu[3], Mark C. M. van Loosdrecht[3] & Kjetill Østgaard[1]*
[1]*Department of Biotechnology, Norwegian University of Science and Technology NTNU, N-7491 Trondheim, Norway*
Tel.: +47 73 59 40 68. Fax +47 73 59 12 83. E-mail: ostgaaard@chembio.ntnu.no
[2]*Department of Ecological Microbiology, BITOEK, University of Bayreuth, Dr.-Hans-Frisch-Str. 1–3, D-95440 Bayreuth, Germany*
[3]*Department of Biochemical Engineering, Delft University of Technology, Kluyver Laboratory for Biotechnology, Julianalaan 67, NL 2628 BC Delft, The Netherlands*
*(*Author for correspondence)*

Key words: nitrification, immobilisation, whole cell hybridisation, multidimensional modelling

Abstract

Nitrifying activated sludge from natural domestic sewage was entrapped in hydrogel beads, which were subsequently enriched for nitrifiers in a continuous stirred tank reactor (CSTR). Fluorescently labelled, 16S rRNA-targeted oligonucleotide probes specific for ammonia and nitrite oxidisers were used in combination with DAPI staining to monitor the selectivity of the enrichment process. The growth of both nitrifying and heterotrophic bacteria was more pronounced in the periphery of the beads, leading to a biofilm-like stratification of the biomass during the enrichment. Quantitatively, the relative number of nitrifiers increased from 20% immediately after immobilisation up to 64% after 30 days, but decreased again due to extensive heterotrophic growth. These changes were accompanied by an increase in nitrifying activity for about 30 days, whereupon it reached a stable level. This selective enrichment was mathematically modelled by applying finite difference techniques to the diffusion-reaction mass balances of all soluble substrates relevant in the nitrification process. To model biomass growth and spreading, balanced by both decay and detachment at the surface of the beads, the differential methods were combined with a descrete cellular automaton approach. The spatially two-dimensional model was used to calculate radial concentration profiles within a gel bead, as well as to estimate the corresponding total activity of the reactor. Qualitatively, this model could simulate all essential aspects observed experimentally. However, more and better population data as well as independent estimates of decay and hydrolysis rates are needed to refine and verify the quantitative model. In conclusion, even in the absence of an external carbon source and with excess ammonium, it was only possible to obtain a moderate enrichment of nitrifying cells compared to heterotrophs. Under long-term cultivation, the biofilm-like structure developed in the outer gel layers led to a vigorous competition between auto- and heterotrophs for space, and thereby, access to oxygen. FISH analysis in combination with mathematical modelling constitute a suitable toolbox for analysing the population dynamics and biocatalytic performance of such an ecosystem based on lithoautotrophic primary production.

Abbreviations: COD – chemical oxygen demand; CSTR – continuous stirred tank reactor; DAPI – 4′,6-diamidino-2-phenylindole; EDTA – ethylenedinitrilo tetraacetic acid; FISH – fluorescence *in situ* hybridisation; HRT – hydraulic retention time; PEG – polyethylene glycol; PVA – polyvinyl alcohol; PVA-SbQ – polyvinyl alcohol with stilbazolium groups

Introduction

Microbial community analysis has been identified as the key to the design of biological wastewater treatment systems (Cloete & Muyima, 1997). In the last years, a battery of molecular techniques has been developed to study microbial ecology in general and community structures in particular (Stahl, 1997; Wagner & Amann, 1997; Burlage et al., 1998; Atlas & Bartha, 1998). Specific bacterial groups in complex open communities such as activated sludge may be detected directly by fluorescence *in situ* hybridisation (FISH), using 16S rRNA-targeted oligonucleotide probes (Stahl & Amann, 1991; Amann et al., 1995; Wagner & Amann, 1997). For instance, by using fluorescent labelled probes specific for ammonia and nitrite oxidisers, the spatial distribution of nitrifiers in a biofilm may be evaluated by *in situ* hybridisation (Wagner et al.,1996; Mobarry et al., 1996; Schramm et al., 1998a).

According to Atlas & Bartha (1998), understanding the structure and functioning of an ecosystem requires and necessitates quantitative information. When microbial ecosystems are applied as catalysts in biological wastewater treatment, a proper quantitative description can only be obtained by complex mathematical models, such as the standard models applied for activated sludge systems (Henze et al., 1995; Gujer et al., 1999). A fundamental parameter in those biokinetic models is the biomass concentration of the particular microbial population involved in each particular process. The validity of such models cannot be verified as long as those fundamental factors remain unknown. Specific populations identified by FISH may possibly be quantified by counting, and compared to total bacterial numbers simply obtained by staining with the DNA-intercalating dye 4,6-diamidino-2-phenylindole (DAPI) to estimate their relative abundance.

The macroscopic performance of such a reactor will depend on transport processes as well as those of the bioconversion. Modelling biofilm processes (Characklis & Marshall, 1990) thus becomes far more complicated than well-mixed sludge systems, particularly after it has been realised that biofilms cannot be considered as simple one-dimensional diffusive systems. However, a two- or three-dimensional model of biofilm growth and structure may be obtained by applying a differential-discrete approach as described by Picioreanu et al. (1999).

Biological N removal depends on a well-functioning nitrification step. The mesophilic lithoautotrophic bacteria involved have low maximal growth rates, 0.5–1 d^{-1} (Henze et al., 1997), and may, therefore, easily be lost in systems with an insufficient sludge age. A prolonged retention may be obtained in a variety of immobilised systems. At the same time, their metabolic independence make them rather insensitive to rapid high-yield organoheterotrophic growth, unless there is a competition for access to oxygen. The nitrification step of biological N removal thus represents a case of interest for combining the two approaches mentioned above, that is the molecular gene probe approach of quantitative FISH analysis and the mathematical approach of multi-dimensional modelling.

Gel entrapment may be used for retention to obtain prolonged sludge age, and thereby enhanced nitrification. Until now, only polyethylene glycol (PEG) cubes of the Pegasus type (Tanaka et al., 1996; Emori et al., 1996) has been applied in full scale wastewater treatment plants (Kyosai & Takahashi, 1996). However, extensive research has also been performed to develop alternative gelling systems suitable for bead production (Wijffels & Tramper, 1995; Wijffels et al., 1996; Leenen et al., 1996; Vogelsang et al., 1997, 2000). As an experimental model system, a spherical bead is obviously simpler to analyse than a cube, particularly when diffusive transport is the rate-limiting process. In any case, in a full scale plant or a lab model ecosystem, a significant fraction of the biomass at any stage of the treatment process may possibly be heterotrophic organisms. A sufficient selection pressure has, therefore, to be maintained to maintain a significant nitrifying activity.

In this preliminary study, starting out with activated sludge from domestic sewage, we used FISH with 16S rRNA-targeted oligonucleotide probes to monitor selective enrichment and to determine the spatial distribution of nitrifiers in gel beads. These experimental results are compared to computer modelled population distributions and estimated overall activity of the same system.

Materials and methods

Materials

The sodium alginate and polyvinyl alcohol with stilbazolium groups (PVA-SbQ) that were used are described in detail by Vogelsang et al. (1997). The nitrification medium had the following composition

(Østgaard et al., 1994): 0.4 g l^{-1} K_2HPO_4, 1.0 g l^{-1} $NaHCO_3$, 25 mg l^{-1} $MgSO_4 \cdot 7H_2O$, 15 mg l^{-1} $CaCl_2 \cdot 2H_2O$, 2.0 mg l^{-1} $FeCl_2 \cdot 4H_2O$, 5.5 mg l^{-1} $MnCl_2 \cdot 4H_2O$, 0.68 mg l^{-1} $ZnCl_2$, 1.2 mg l^{-1} $CoCl_2 \cdot 6H_2O$, 1.2 mg l^{-1} $NiCl_2 \cdot 6H_2O$, 28 mg l^{-1} EDTA, and concentrations of NH_4^+ varying from 25.0 mg N l^{-1} to 125.0 mg N l^{-1}. The components were dissolved in tap water and the pH was adjusted to 7.3. The Tris buffer had in all cases pH 7.3. All chemicals used were of analytical quality.

Preparation of nitrifying sludge for immobilisation

Nitrifying sludge that had been stored frozen in 15% glycerol was reactivated in a 6 l sequence batch reactor at 25 °C and pH 7.3 for three weeks. The reactor was cooled down to 4 °C before the sludge was filtered through a 50–110 μm plankton filter sheet to remove protozoa. Excess sludge on the filter was resuspended in 10 mM Tris buffer, homogenised on a kitchen blender and refiltered through the planktonic sheet. The supernatant was examined in a microscope for presence of protozoa before centrifugation at 2000 rpm for 10 min. The pellet was resuspended in 10 mM Tris buffer and vigorously stirred for 1 h to be homogenised before immobilisation. Unless otherwise stated, the whole immobilisation procedure was carried out at 4 °C.

Gel entrapment

A 13.17% PVA-SbQ water solution was diluted to 10% with the sludge suspension and mixed for 1 h by gentle stirring. A 4% solution of sodium alginate in 10 mM Tris buffer was added in equal amounts to the PVA-SbQ & sludge suspension and stirred gently for another hour. 400 ml of this mixture was added dropwise into a large reservoir of 0.1 M $CaCl_2$ in 10 mM Tris buffer using a suitable device (Klein & Wagner, 1978; Smidsrød & Skjåk–Bræk, 1990) to obtain spherical 5% PVA-SbQ & 2% Na-alginate gel beads with an average diameter of 2.5 mm (Hertzberg et al., 1995; Vogelsang et al., 1997). The beads were kept in this gelling solution and exposed to light from racks of 18 W white light tubes overnight to finish the photocrosslinking of the PVA-SbQ polymer network. The final gel bead volume was 490 ml with a sludge concentration of 42 g wet weight sludge per l gel beads. The whole procedure was carried out at 4 °C.

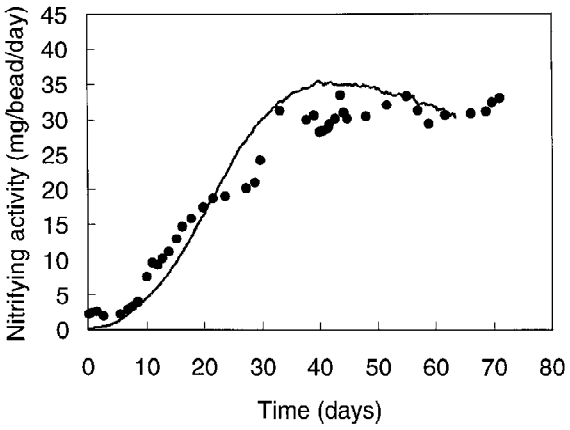

Figure 1. Nitrifying activity, measured as ammonium removal rate, per gel bead in lab reactor during selective enrichment of gel entrapped nitrifiers (•). Continuous curve represents the corresponding activity according to theoretical model (see text).

Lab scale nitrification

The 490 ml of gel beads were used to inoculate a 4.4 l continuous stirred tank reactor (CSTR) for precultivation at 15 °C. The first 1.5 days the reactor was run under batch conditions, switching to a hydraulic retention time (HRT) of 11–17 h for the following 7 days.

For long-term cultivation, 25% of the gel beads were transferred to a 400 ml CSTR, giving a bead volume filling of approximately one third. The aeration was increased stepwise from 1.2 l min^{-1} to 1.5 l min^{-1} at day 16 and to the final flow 2.0 l min^{-1} at day 26, keeping the dissolved oxygen concentration in the range of 4–9 mg O_2 l^{-1}. The HRT was kept at 2–3 h. The reactors were aerated through a 6-cm^3 rectangular glass sintered aquarium filter and agitated by magnetic stirring at 500–600 rpm. The temperature was kept at 15 °C throughout the experiment.

From day 37, the reactor was maintained at roughly similar conditions, but due to an operational failure, the beads had to be transferred to another reactor system at day 66.

Concentrations of ammonium, nitrate and nitrite were determined daily using DrLange Cuvette tests LCK 303, LCK 339 and LCK 341 (DrLange, 1992) in accordance with international standards (DIN 38 406-E5-1, DIN 38402-A51 and DIN 38 405-D 10, respectively). Calculated nitrifying activities were normalised per gel bead.

Fluorescence in situ *hybridisation (FISH)*

Beads were sampled right after immobilisation and at days 30 and 80. The beads were fixed in 4% paraformaldehyde and cut in 10 μm sections using a cryomicrotome. After immobilisation on poly-L-lysine coated slides, the sections were hybridised with fluorescent labelled probes specific for different phylogenetic groups of nitrifiers as indicated in Table 1, and simultaneously stained with 4′,6-diamidino-2-phenylindole (DAPI) for total cell counts. Slides were examined with an Axioplan epifluorescence microscope (Carl Zeiss) equipped with filter sets 01, HQ-CY3 and HQ-CY5. This complete procedure was described in detail by Schramm et al. (1998b). A semi-quantitative estimation of the abundance and spatial distribution of nitrifiers and non-nitrifying organisms in the beads was done by bacterial counts of one representative bead centre-section for each probe at each sampling. The enumeration was carried out by identifying five size categories for colonies and counting size-classified colonies rather than single cells. The outer 300 μm peripheral layer of the beads was enumerated separately from the central core.

Mathematical model

Ecosystem modelling

The combined differential-discrete cellular automaton approach for biofilm modelling is described in detail elsewhere (Picioreanu et al., 1998, 1999). A spatially two-dimensional version of the above model was used in the present study. Soluble components such as substrates are represented in a continuous field, whereas discrete mapping is used for solid components such as biomass. The spatial distribution of substrate is calculated by applying finite difference relaxation methods to the reaction-diffusion mass balance. A biomass density map is determined from direct integration in each grid cell of a substrate-limited growth equation, while spreading and distribution of biomass is modelled by a discrete cellular automaton algorithm.

This approach has previously been successfully applied to model growth of pure cultures in spherical gel beads, as described by Picioreanu et al. (1998). In this model, growth is balanced by a detachment process denoted single-cell release: If the space where the newly formed biomass has to be placed is located outside the carrier sphere, then this microbial cell is simply lost. This approach is considered more realistic in our case, since the colony expulsion observed by Wijffels (1994) in carrageenan gels does not seem to be of significance for the superelastic low gel strength PVA-SbQ gels applied here (Vogelsang et al., 2000).

The gel bead model developed by Picioreanu et al. (1998) was extended to describe a microbial community consisting of three biomass populations; ammonia oxidisers (X_1), nitrite oxidisers (X_2) and heterotrophs (X_3). Correspondingly, a minimum of four substrates had to be included, that is ammonium, oxygen, nitrite, and organic matter expressed as chemical oxygen demand (COD).

The kinetic model of the nitrification process presented below was adapted from Wiesmann (1994), as also applied by Picioreanu et al. (1997). Decay of nitrifiers and growth of heterotrophs were added with parameters close to those found in activated sludge models (Henze et al., 1995; Gujer et al., 1999), as well as the single-cell release biomass detachment described above.

Stoichiometry and kinetics

Three biomass populations and four substrates are considered, applying the symbols X_1: ammonia oxidisers, X_2: nitrite oxidisers and X_3: heterotrophs for biomass, and S_1: ammonia, S_2: oxygen, S_3: nitrite, S_4: COD and S_5: nitrate for dissolved compounds. The stoichiometry of the five microbial processes considered, together with their associated reaction rates r, are as follows:

Growth of ammonia oxidisers:

$$-S_1\frac{Y_{11}}{Y_{12}}S_2+\frac{Y_{11}}{Y_{13}}S_3+Y_{11}X_1=0 \qquad r_1=q_{S1}c_{X1}$$

Growth of nitrite oxidisers:

$$-S_3-\frac{Y_{23}}{Y_{22}}S_2+\frac{Y_{23}}{Y_{25}}S_5+Y_{23}X_2=0 \qquad r_2=q_{S2}c_{X2}$$

Decay of ammonia oxidisers:

$$-X_1+Y_{14}S_4=0 \qquad r_3=k_{d1}c_{X1}$$

Decay of nitrite oxidisers:

$$-X_2+Y_{24}S_4=0 \qquad r_4=k_{d2}c_{X2}$$

Growth of heterotrophs:

$$-S_4-Y_{32}S_2+Y_{34}X_3=0 \qquad r_5=q_{S3}c_{X3}$$

Table 1. Oligonucleotide probes used to identify nitrifiers in the 5% PVA-SbQ & 2% alginate gel beads

Probe	Specificity	Reference
NSO190	Ammonia oxidisers of β-Proteobacteria	Mobarry et al. (1996)
NSV443	Genus *Nitrosospira*, including *Nitrosovibrio, Nitrosolobus*	Mobarry et al. (1996)
NSM156	Genus *Nitrosomonas*	Mobarry et al. (1996)
NIT3	Genus *Nitrobacter*	Wagner et al. (1996)
cNIT3	Unlabelled competitor for NIT3	Wagner et al. (1996)
NSR826	Most freshwater *Nitrospira* sp.	Schramm et al. (1998b)

The substrate conversion kinetics is expressed as specific q rates modelled by Monod equations with double limitation by electron donor species as well as acceptor (oxygen). If the N substrates are present in high concentrations, both NH_3 and HNO_2 could also be inhibitors, represented in the following equations as described by Picioreanu et al. (1997):

$$q_{S1} = q_{m,S1} c_{X1} \cdot \frac{c_{S1}}{K^*_{S1} + c_{S1} + \frac{c^2_{S1}}{K^*_{I1}}} \cdot \frac{c_{S2}}{K_{S2,1} + c_{S2}}$$

$$q_{S2} = q_{m,S2} c_{X2} \cdot \frac{c_{S3}}{K^*_{S3} + c_{S3} + \frac{c^2_{S3}}{K^*_{I3}}} \cdot \frac{c_{S2}}{K_{S2,2} + c_{S2}}$$

$$q_{S3} = q_{m,S3} c_{X3} \cdot \frac{c_{S4}}{K_{S4} + c_{S4}} \cdot \frac{c_{S2}}{K_{S2,3} + c_{S2}}$$

In accordance with Wiesmann (1994), the saturation (K_{Si}) and inhibition (K_{Ii}) concentrations can be transformed to obtain concentrations of the corresponding neutral species by applying:

$$K^*_{S1} = \frac{K_{S1} K_a}{10^{\mathrm{pH}}},\ K^*_{I1} = \frac{K_{I1} K_a}{10^{\mathrm{pH}}},$$
$$K^*_{S3} = K_{S3} K_b 10^{\mathrm{pH}},\ K^*_{I3} = K_{I3} K_b 10^{\mathrm{pH}}$$

The actual stoichiometric and kinetic parameters and parameter values that were used in the model simulations are summarised in Table 2. This model was applied to calculate radial concentration profiles within a gel bead as well as to estimate the corresponding total overall activity of the reactor.

Results

Reactor performance

Figure 1 shows the nitrifying activity, measured as ammonium removal rate, for the first 70 d of cultivation. Nitrite accumulation was insignificant during the recorded period (results not included). According to measurements, a pseudo-steady state of maximal activity was apparently reached within 35 d. This is in accordance with the characteristic enrichment response pattern observed earlier in ammonium-enriched domestic wastewater (Vogelsang et al., 1997) as well as during regeneration of frozen and/or dried beads after storage (Vogelsang et al., 1999).

The reactor was maintained at roughly stable conditions, but due to an operational failure, the beads had to be transferred to another reactor system at day 66. As expected for an oxygen transfer rate-limited system (Vogelsang et al., 1997), this lead to transient changes in total activity (<25%) not included in the graph. Beads were sampled right after immobilisation (day 0) and at days 30 and 80 for FISH analysis (Table 3).

In situ *identification of nitrifiers*

To avoid the green autofluorescence of the gel material PVA-SbQ (spectra not included), red fluorochromes such as CY3 and CY5 had to be applied for probe labelling to obtain reliable visualisation of cells (Fig. 2). This restricted the number of applicable dyes and probe combinations.

The dominant ammonia oxidisers in all samples were *Nitrosospira* sp.; their numbers correlated well with the cell numbers of all ammonia oxidisers as detected by probe NSO190 (Table 1). In agreement with these results, no members of the genus *Nitrosomonas* could be detected, although it has been reported

Table 2. Model parameters

Parameter	Symbol	Ammonia ox.	Nitrite ox.	Heterotrophs	Units
Kinetics		*i = 1*	*i = 2*	*i = 3*	
Maximum specific consumption rate	$q_{m,Si}$	$0.75{\cdot}10^{-4}$	$3.178{\cdot}10^{-4}$	$0.9{\cdot}10^{-4}$	s^{-1}
Decay constant	k_{di}	$2{\cdot}10^{-6}$	$1{\cdot}10^{-6}$	–	s^{-1}
Monod saturation constant of NH_3	K_{S1}	$2.8{\cdot}10^{-5}$	–	–	kg m^{-3}
Monod saturation constant of HNO_2	K_{S3}	–	$3.2{\cdot}10^{-8}$	–	kg m^{-3}
Monod saturation constant of O_2	$K_{S2,i}$	$0.3{\cdot}10^{-3}$	$1.1{\cdot}10^{-3}$	$0.2{\cdot}10^{-3}$	kg m^{-3}
Monod saturation constant of COD	K_{S4}	–	–	$20{\cdot}10^{-3}$	kg m^{-3}
Inhibition constant of NH_3	K_{I1}	$540{\cdot}10^{-3}$	–	–	kg m^{-3}
Inhibition constant of HNO_2	K_{I3}	–	$0.26{\cdot}10^{-3}$	–	kg m^{-3}
Growth yield on ammonia	Y_{i1}	0.147	–	–	kg VSS X kg^{-1} N–NH_3
Growth yield on oxygen	Y_{i2}	0.046	0.039	–	kg VSS X kg^{-1} O_2
Growth yield on HNO_2	Y_{i3}	0.147	0.042	–	kg VSS X kg^{-1} N–HNO_2
Growth yield on COD	Y_{i4}	–	–	0.5	kg VSS X kg^{-1} COD
Oxygen consumption during COD oxidation	Y_{32}	–	–	0.33	kg $O_2$$kg^{-1}$ COD
COD yield from decay	Y_{i4}	1.33	1.33	–	kg COD kg^{-1} VSS X_i
Mass transfer					
Diffusion coefficient of NH_4^+ in water	D_{S1}	$1.4{\cdot}10^{-9}$			m^2 s^{-1}
Diffusion coefficient of O_2 in water	D_{S2}	$1.6{\cdot}10^{-9}$			m^2 s^{-1}
Diffusion coefficient of NO_2^- in water	D_{S3}	$1.4{\cdot}10^{-9}$			m^2 s^{-1}
Diffusion coefficient of COD in water	D_{S4}	$0.4{\cdot}10^{-9}$			m^2 s^{-1}
Geometry and operation					
Total reactor volume	V_R	0.4			l
Bead diameter		$2.5{\cdot}10^{-6}$			m
Fraction from maximum concentration in each grid cell inoculated		0.2	0.2	0.2	
Maximum concentration of bacteria in colony	$c_{Xm,i}$	50.0	40.0	50.0	kg m^{-3}
PH		7.3			
Temperature	T	15			°C
Concentration of NH_4^+ in bulk liquid	C_{S1}	$10{\cdot}10^{-3}$			kg m^{-3}
Concentration of O_2 in bulk liquid	C_{S2}	$3.5{\cdot}10^{-3}$			kg m^{-3}
Concentration of NO_2^- in bulk liquid	C_{S3}	$0.5{\cdot}10^{-3}$			kg m^{-3}
Concentration of COD in bulk liquid	C_{S4}	$1.5{\cdot}10^{-3}$			kg m^{-3}

Table 3. Calculated activities, cell densities and specific activity of ammonia oxidisers (NSV443) and nitrite oxidisers (NIT3 + NSR826) inside the gel beads

Time	Ammonia oxidising bacteria			Nitrite oxidising bacteria		
	Activity [μg N d^{-1} $bead^{-1}$]	Cell density [cells $bead^{-1}$]	Apparent specific activity [pg N d^{-1} $cell^{-1}$]	Activity [μg N d^{-1} $bead^{-1}$]	Cell density [cells $bead^{-1}$]	Apparent specific activity [pg N d^{-1} $cell^{-1}$]
0	0.09	$0.5{\cdot}10^7$	0.018	0.03	$<0.1{\cdot}10^7$	>0.03
30 d	1.0	$5{\cdot}10^7$	0.020	1.0	$4{\cdot}10^7$	0.025
80 d	1.5	$8{\cdot}10^7$	0.019	1.5	$4{\cdot}10^7$	0.038
	1.8	$6{\cdot}10^7$	0.030	1.8	$6{\cdot}10^7$	0.030

as the generally most abundant ammonia oxidiser in wastewater treatment plants (Wagner et al., 1995; Mobarry et al., 1996; Schramm et al., 1998b). *Nitrobacter* sp. dominated among the nitrite oxidisers, however, a few cells of the nitrite oxidiser *Nitrospira* sp. were also recognised.

After cultivation, most nitrifiers formed typically dense clusters of hundreds and thousands of cells, as illustrated in Figure 2. The ammonia and nitrite

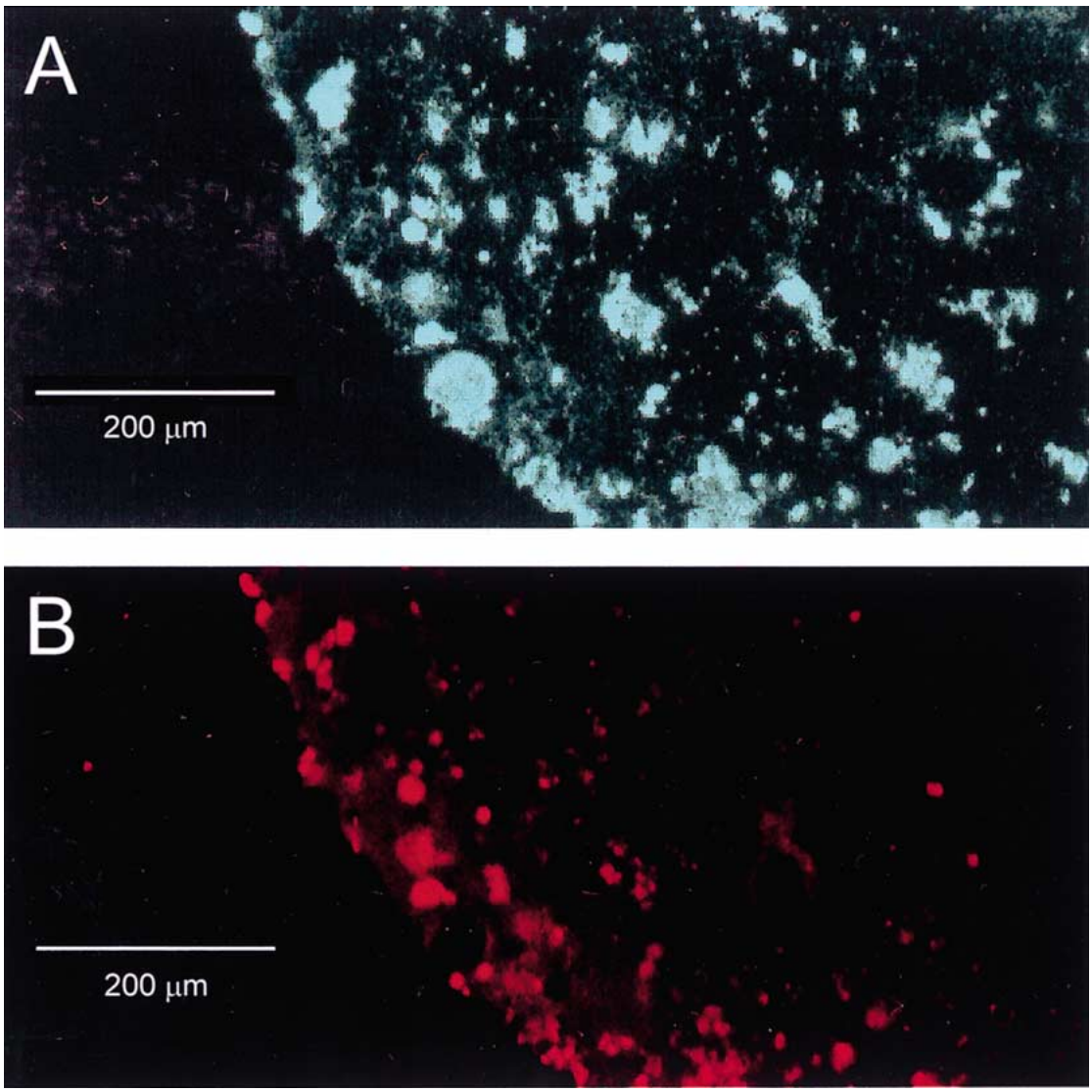

Figure 2. Spatial distribution of biomass and nitrifiers in a gel bead at day 80: (A) DAPI staining of the bead showing all bacteria; (B) same microscope field after FISH staining with probes NSV443 and NIT3, both labelled with red fluorescent CY3. Bars = 200 μm.

oxidisers appeared in separate, but often closely associated colonies. There was a clear cell size difference between the ammonia oxidisers and nitrite oxidisers, with the ammonia oxidisers generally at the order of twice as big in linear dimensions (observations not included).

Selective enrichment monitored by FISH

As shown in Figure 3, total cell counts after DAPI staining revealed a strong growth in biomass that was even more pronounced at the periphery of the beads. At the end of the experiment, a biofilm-like structure had developed, with the dominant biomass concentrated within the outer 100-μm layer of the gel of the beads.

The FISH data displayed in Table 3 and Figure 4 showed a 10-fold growth in the nitrifying biomass during the first 30 days, in the central core as well as the peripheral part of the beads. This is similar to the increase in the nitrifying activity per bead, approaching an apparent steady state (Fig. 1). During the next 50 d, growth of nitrifiers was only observed in the outer layer (70% increase), whereas the numbers of nitrifiers in the inner part of the beads decreased by approx-

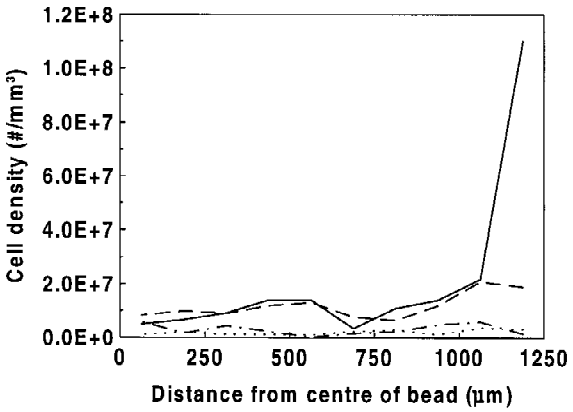

Figure 3. Radial distribution from centre of bead of all bacteria estimated by total counts after staining with DAPI. Line codes for days after inoculation: Dotted = day 0, dashed and dotted = day 8, broken = day 30, solid = day 80.

imately one third (Fig. 4). Except for the inoculum directly after immobilisation at day 0, the number of ammonia oxidisers and the number of nitrite oxidisers appeared to be within the same order of magnitude throughout the experiment, and the apparent specific activity did not change dramatically (Table 3).

The fractional ratio of nitrifying bacteria relative to all bacteria increased from 20% directly after immobilisation to 64% at day 30. Despite the strictly inorganic medium used, other non-nitrifying organisms, probably a variety of heterotrophic bacteria, were able to survive and proliferate in the beads. The major part of this growth occurred in the outer 300-μm layer (Fig. 4). Therefore, even if there was an approximately 30% increase in the nitrifying biomass from day 30 to 80, the fractional ratio of nitrifiers was reduced to 35% during this period. Thus, only a moderate enrichment of nitrifiers was actually achieved over the whole period.

Model simulations

The characteristic properties of the applied model are summarised in Figures 5–8. The corresponding total nitrifying activity calculated per bead is included as the curve shown in Figure 1.

Figure 5 gives a two-dimensional visualisation of the growth of the three populations of the model. Clearly, a stratification of the biomass in large nitrifying and heterotrophic colonies can be seen already at day 20, leading to an outer biofilm-like peripheral layer of the beads. As illustrated, oxygen deficiency promoted this stratification.

Figure 6 presents the quantitative radial oxygen profiles, as well as ammonia, nitrite and COD. Clearly, oxygen should be considered as the mutual limiting substrate for the 3 different populations, leading to ecological competition for space between the organoheterotrophs and litoautotrophs in the aerobic outer layers of the modelled gel bead.

Figure 7 illustrates the resulting radial microbial community distribution. There was a notable difference in the biofilm layer thickness between the three populations, with the dominant parts of the ammonia oxidisers, nitrite oxidisers and heterotrophs distributed in layers of approximately 100 μm, 150 μm and 300 μm thickness, respectively. Noteworthy is also the substantial difference in the maximum average biomass concentrations of ammonia oxidisers compared to nitrite oxidisers, basically reflecting the difference in their growth yields.

Figure 8 finally shows the resulting population densities calculated for the central core compared to outer peripheral layer of the beads for a more direct comparison with the FISH data of Figure 4. Please note that the model operates with biomass concentrations in kg m^{-3}, while the FISH analysis was based on numerical counting. In the central core, the model showed some prolonged heterotrophic growth, as observed experimentally, but also estimated a decrease in the number of nitrifiers in the central core already from around day 15 (Fig. 8) that was not experimentally verified (Fig. 4).

In the outer layer, the model predicted a growth pattern (Fig. 8) that resembled the experimental community analysis (Fig. 4) quite well for the enrichment period of the first 30 days. The observed sustained heterotrophic growth even after reaching the apparent steady state nitrifying activity around day 35 (Fig. 1) could also be modelled. According to the model, approximately 57% of the biomass would be heterotrophs at day 30, increasing to approximately 85% at day 60 (Fig. 8). The absolute amount of nitrifying biomass in the outer layer was actually estimated to decrease again from day 30 to 60 (Fig. 8). As a result, the theoretically modelled activity never reached a stable steady state, but rather started to fall again after passing a maximum around day 40, as shown above in Figure 1.

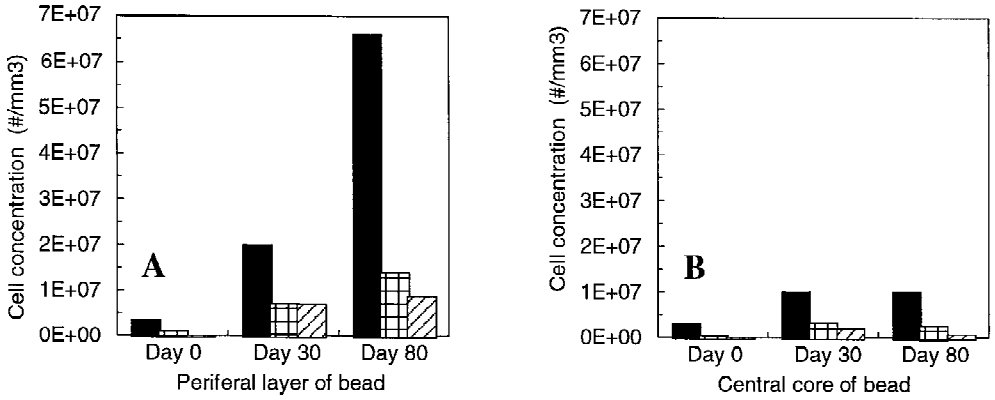

Figure 4. Density of DAPI-stained bacteria ■, *Nitrosospira* sp. ⊞, and *Nitrobacter* sp. ▨ in the outer 300 μm peripheral layer (A) compared to the inner central core (B) of the beads as estimated by FISH and DAPI staining and counting.

Discussion

FISH reliability

There is a risk in doing a direct comparison between the *phenotypical* nitrifying activity and the *phylogenetic* similarities within the group of known nitrifiers identified by the applied rRNA probes. The inherent limitations and current obstacles related to probe specificity, as discussed in detail by Amann et al. (1995) and Oerther et al. (1999), should also be taken into account.

Furthermore, the rough numerical estimation and the low resolution in the given spatial distribution of the nitrifiers restricted this investigation to a rather semi-quantitative evaluation of the dynamic progress of the growth of nitrifiers inside the beads (Fig. 4). Still, the results may demonstrate essential potentials and pitfalls in combining FISH and activity measurements when analysing ecological community structures applied as biocatalysts in open environmental systems.

Model flexibility

As shown above, our computer model could easily be adapted to the basic recorded pattern of heterotrophic growth based on nitrifying autotrophic primary production as the sole carbon source (Figs 4 and 8), as well as the corresponding macroscopic activity of the reactor system (Fig. 1). However, the limited FISH data available in this particular case (Fig. 4) was clearly insufficient for a full and proper model verification. In addition, even this highly simplified model behaviour will depend on the quality of a large variety of data and necessary parameters (Table 2). This has to be taken into consideration when evaluating the total outcome. As always, the macroscopic balance of the system will depend on conversion as well as transport processes.

Conversion is determined by the stoichiometry and biokinetic model presented above, with the parameters given in Table 2. In this particular case, decay is a crucial factor as the limiting process and only supply of organic carbon to the ecosystem. Reliable data are scarce, particularly for a system like this where grazing by proto- and metazoa, normally dominant in aerobic systems, could no longer be observed. In the rough calculations presented, decay of heterotrophs has simply been neglected, while decay at 1–2 10^{-6} s^{-1} was assigned to the nitrifiers (Table 2). These values may easily be adjusted. Far more important is the simplified assumption that all decayed material becomes readily available COD substrate directly. A refined model may include hydrolysis as the rate-limiting step instead, that is a COD transfer from autotrophic biomass to available organic substrate proportional to the local concentration of (presumably hydrolytic) heterotrophs. In such a case, the loss of nitrifiers would become much higher in the outer layers than in the central core, which would bring the model (Fig. 8) even closer to the data observed (Fig. 4). It is considered less important to also include an inert fraction in this revision. A refined model may also be more easily adjusted to the apparent long-term steady state nitrification observed (Fig. 1).

Transport is simply diffusive and simple to calculate due to the spherical geometry of the gel beads. Previous experimental studies (Vogelsang et al., 1997)

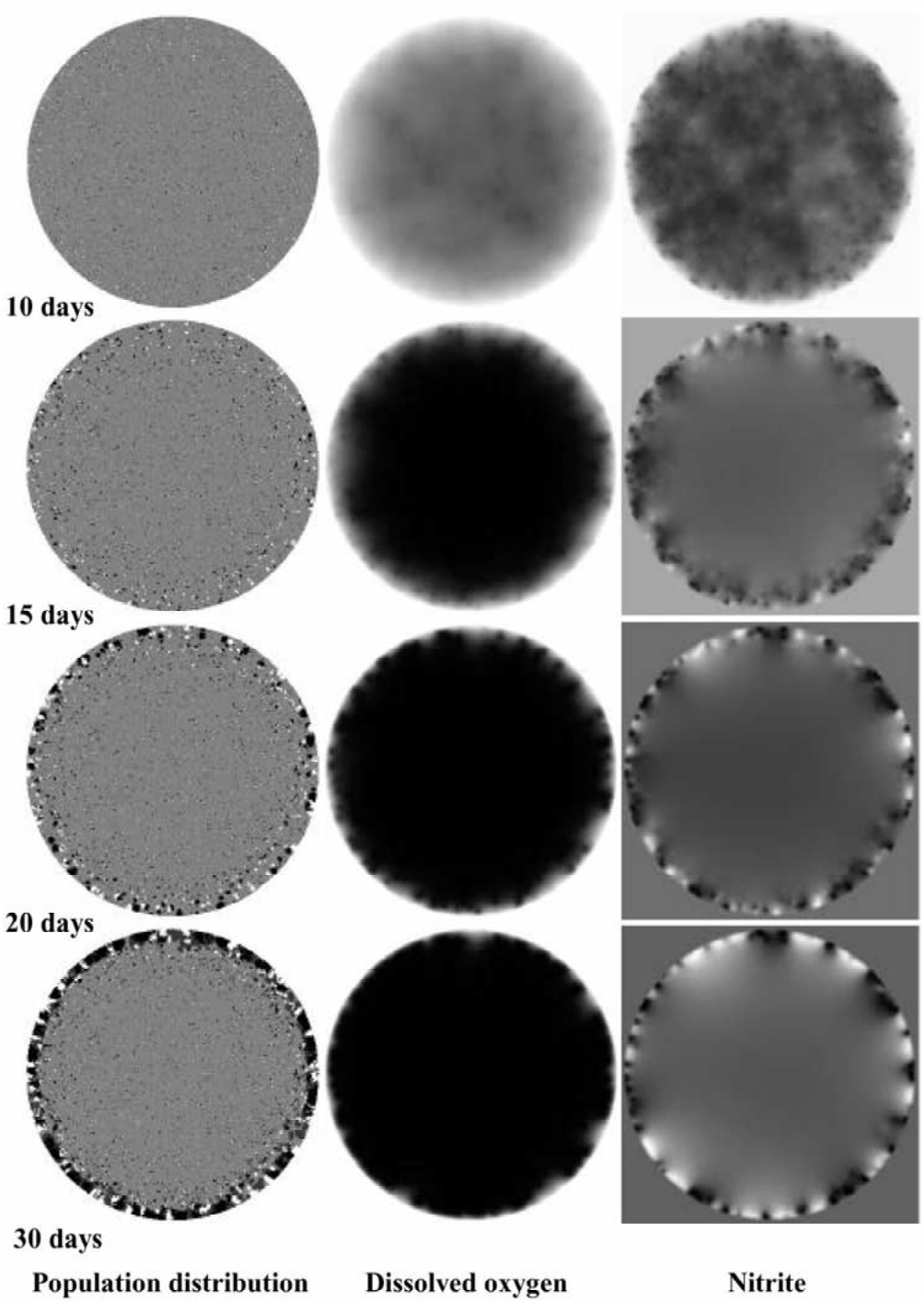

Figure 5. Spatial distribution of biomass and substrates at days 10, 15, 20 and 30 as simulated by mathematical model. Colour codes for populations: Black = ammonia oxidisers, white = nitrite oxidisers, dark grey = heterotrophs, and light gray is the gel carrier. For substrates, a grey scale was calibrated over the whole domain for each graph, ranging from black showing the minimum to white showing to maximum concentration.

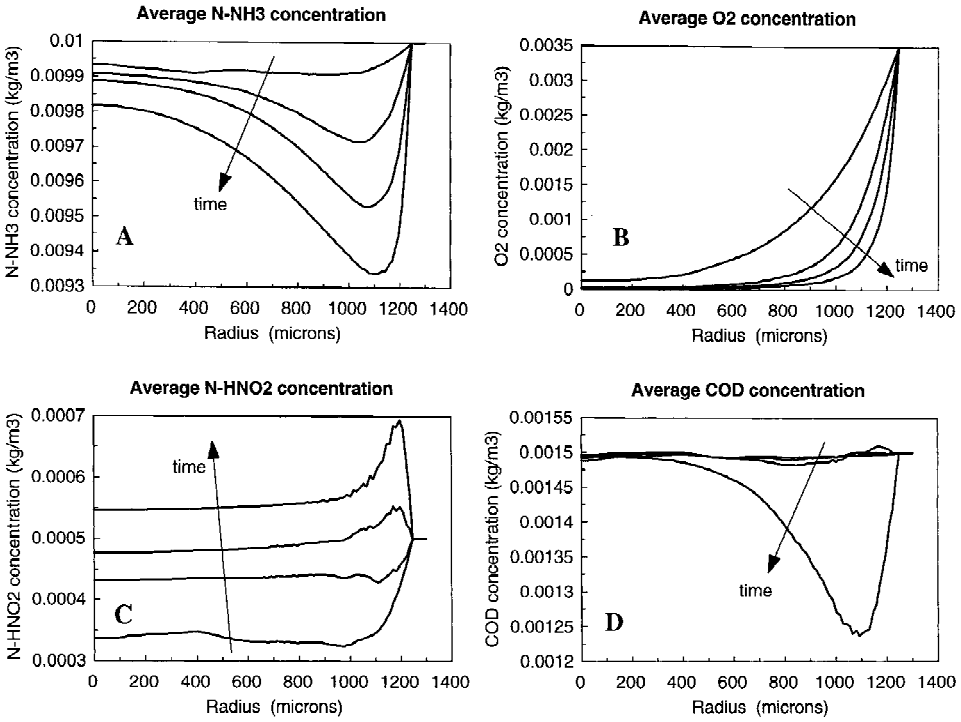

Figure 6. Average radial distribution from centre of bead of dissolved compounds at days 10, 15, 20 and 30 as simulated by mathematical model. (A) N–NH_3, (B) dissolved O_2, (C) N–HNO_2, and (D) COD concentrations. Time arrow indicates direction of progress.

as well as the model simulated dissolved oxygen profiles in the beads (Fig. 5) clearly showed that oxygen should be considered as the rate limiting substrate. The active nitrifying biofilm thickness will depend on the oxygen penetration depth, and the actual bulk liquid oxygen concentration would be the most important factor to control the overall activity in the reactor. Dissolved oxygen was not continuously recorded during the whole experiment, and may have varied within a factor of 2. Better control and better data is obviously essential for a more detailed modelling. Assuming constant conditions, the model gave still a reasonable fit to the somewhat scattered activity data as shown in Figure 1.

Model vs. data

The relative amounts of the three populations, calculated from the biomass concentrations (kg m^{-3}) in the model simulations or from the observed experimental cell densities (number of cells per mm^3), cannot be compared directly because of the relatively large variations in cell sizes. As observed in the microscope, our dominant ammonia oxidisers were clearly larger than the nitrite oxidisers, in accordance with literature reporting *Nitrosospira* cells as rods or cylinders of 1.5–2.5 μm length and 0.8–1.0 μm width (Watson, 1971), while *Nitrobacter* are reported as shorter and rather dense rods of 1.0–2.0 μm length and 0.8 μm width (Murray & Watson, 1965; Watson & Mandel, 1971). Due to the semi-quantitative approach applied, we do not have exact and reliable data suitable for a direct recalibration between community structure expressed as experimental cell numbers (Fig. 4) and expressed as model biomass (Fig. 8). However, at the maximal enrichment observed, that is at day 30, the model estimated biomass per biomass fraction of nitrifiers therefore turned out to be somewhat lower, approx. 43%, than the experimental number per number ratio of 64%, as expected.

During the growth and enrichment phase of the first month, a biofilm-like structure developed at a rate illustrated by the experimental data of Figure 3, with the corresponding model simulation shown in Figure 7. While only two thirds of the total community was found experimentally in the outer 300 μm layer at day 30 (Fig. 4), the model estimated that more than 90% would be in this layer (Fig. 8). For the nitrifying biomass the ratios were 73 and 97%, re-

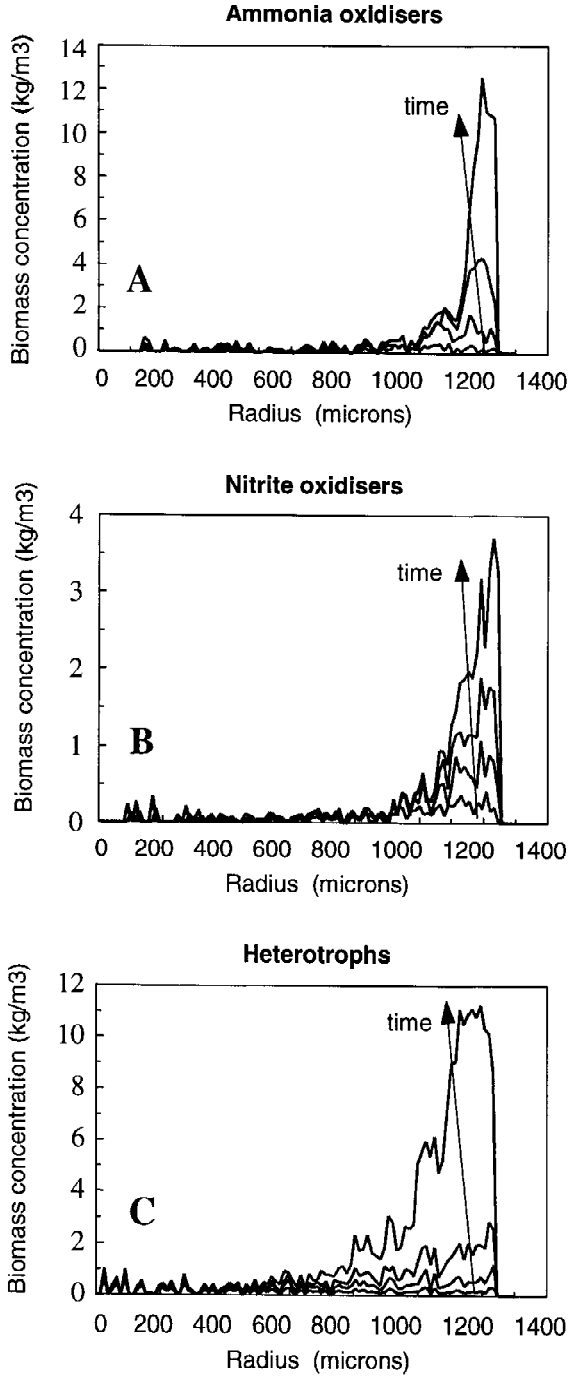

Figure 7. Average radial distribution from centre of bead of different populations at days 10, 15, 20 and 30 as simulated by mathematical model. (A) ammonia oxidisers, (B) nitrite oxidisers, (C) heterotrophs. Time arrow indicates direction of progress.

spectively. This inconsistency is probably connected to differences in the initial biomass distribution. While the model was initiated with evenly distributed single cells, FISH analysis revealed large aggregates even in the newly made gel beads. It is experimentally difficult to avoid such aggregates when immobilising activated sludge without killing the microorganisms during the homogenisation step.

The experimental activity data indicated a distinct steady state from around day 30 onwards (Fig. 1). The continued high nitrification activity was also confirmed by the FISH data for day 80, showing a significant increase in the nitrifying population since day 30 (Fig. 4). This occurred even when the heterotrophs strongly proliferated in the beads. The model simulation, however, did not show such a steady state activity. After reaching an optimum around day 40 (Fig. 1), the activity declined due to a rapid loss of nitrifiers caused by decay as well as competition for space in outer layers of the beads. Hence, decayed nitrifiers served as food for a rapidly spreading heterotrophic population, which in turn, pushed the nitrifiers out of the bead by the single-cell release detachment process implemented in the model. By tuning and refining the decay and hydrolysis parts of the model, a better fit should obviously be obtainable.

Despite the strictly inorganic medium used, non-nitrifying heterotrophic bacteria were able to survive and proliferate in the beads. Some organic carbon was initially present due to the sludge used for inoculation as well as the alginate of the gel matrix that tends to be lost (Vogelsang & Østgaard, 1996; Vogelsang et al., 1997). In both cases, this contamination must be hydrolysed to become available. It is reasonable that decay products and extracellular polymeric substances from the nitrifying populations were a more dominant carbon source for the long-term heterotrophic growth observed.

General aspects

The gel entrapment and model system described here may be applied directly for scaled up moving bed reactors when found economically feasible (Vogelsang et al., 1997, 1999, 2000), or applied as a simplified lab model system of relevance also for other non-spherical gel entrapped or biofilm systems as discussed above.

This initial and preliminary study is only meant to illustrate the potential of a structured and combined use of FISH analysis and mathematical modelling. Obviously, more and better population data as well as independent studies and estimates of decay and hydrolysis are needed to refine and verify a final quantitative

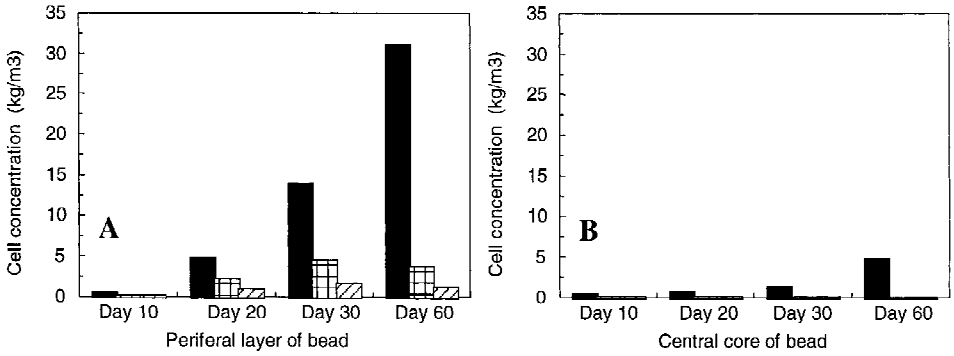

Figure 8. Average densities of all bacteria ■, ammonia oxidisers ⊞, and nitrite oxidisers ▨ in the outer 300 μm layer (A) compared to the inner central core (B) of the beads as simulated by mathematical model.

model. The next step would then be to test out the ecosystem response to changes in external conditions such as organic loading and aeration, not just in steady state, but also to model transient adaptation to step changes as well as pulsed conditions.

Conclusions

The gel bead ecosystem constitutes a microbial community suitable for quantitative analysis and modelling due to its simple spherical geometry and the purely diffusive transport.

FISH analysis in combination with suitable mathematical models as well as standard measurements of the macroscopic reactor performance constitute a suitable toolbox for analysis of the population dynamics and biocatalytic performance of such an ecosystem.

Even in the absence of an external carbon source and with excess ammonium, it was only possible to obtain a moderate enrichment of nitrifying cells compared to heterotrophs. Under long-term cultivation, a biofilm-like structure developed in the outer layers, with a vigorous competition for space, and thereby access to oxygen, between auto- and heterotrophs. The differential-discrete approach presented here was able to model such an ecosystem based on litoautothrophic primary production.

Acknowledgements

We thank R. Amann, Max-Planck-Institute for Marine Microbiology for his support with the FISH analysis. This work was in part supported by the Max Planck Society, and by the Deutsche Forschungsgemeinschaft (SFB 411), as well as the Norwegian Research Council (NFR).

References

Amann, R. I., K. Ludwig & K.-H. Schleifer, 1995. Phylogenetic identification and *in situ* detection of individual microbial cells without cultivation. Microbial Rev. 59: 143–169.

Amann, R., H. Lemmer & M. Wagner, 1998. Monitoring the community structure of wastewater treatment plants: a comparison of old and new techniques. FEMS Microbiol. Ecol. 25: 205–215.

Atlas, R. M. & R. Bartha, 1998. Quantitative ecology: numbers, biomass, and activities. In Atlas, R. M. & R. Bartha, Microbial Ecology: Fundamentals and Applications, Benjamin/Cummings Science Publishing, Menlo Park CA: 218–263.

Burlage, R. S., R. M. Atlas, D. Stahl, G. Geesey & G. Sayler (eds), 1998. Techniques in Microbial Ecology. Oxford University Press, New York: 468 pp.

Charaklis, W. G. & K. C. Marshall (eds), 1990. Biofilms. John Wiley & Sons, New York: 796 pp.

Cloete, T. E. & N. Y. O. Muyima, 1997. Microbial Community Analysis: the Key to Design of Biological Wastewater Treatment Systems. IAWQ Scientific and Technical Report No. 5. University Press, Cambridge: 98 pp.

DrLange, 1992. Handbook of Photometrical Operation Analysis. Dr Bruno Lange GmbH, Berlin: 323 pp.

Emori, H., K. Mikawa, M. Hamaya, T. Yamaguchi, K. Tanaka & T. Takeshima, 1996. Pegasus. Innovative biological nitrogen removal process using entrapped nitrifiers. In Wijffels, R. H., R. M. Buitelaar, C. Bucke & J. Tramper (eds), Immobilized Cells: Basics and Applications. Elsevier Science Publishers, Amsterdam: 546–555.

Gujer, W., M. Henze, T. Mino & M. van Loosdrecht, 1999. Activated sludge model no. 3. Wat. Sci. Technol. 39: 183–193.

Henze, M., W. Gujer, T. Mino, T. Matsuo, M. C. Wentzel & G. v. R. Marais, 1995. Activated Sludge Model No. 2 . IAWQ Scientific and Technical Report No. 3. IAWQ, London: 32 pp.

Henze, M., P. Harremoës, J. la Cour Jansen & E. Arvin, 1997. Wastewater Treatment. Biological and Chemical Processes. Springer-Verlag, Berlin Heidelberg: 383 pp.

Herzberg, S., E. Moen, C. Vogelsang & K. Østgaard, 1995. Mixed photo-crosslinked polyvinyl alcohol and calcium-alginate gels for cell entrapment. Appl. Microbiol. Biotechnol. 43: 10–17.

Klein, J. & F. Wagner, 1978. Immobilized whole cells. In Behrens, D. & K. Fischbeck (eds), Biotechnology. Proceedings of the First European Congress on Biotechnology, 25–29 September 1978 (Dechema Monographien No. 82). Verlag Chemie, Weinheim: 142–164.

Kyosai, S. & M. Takahashi, 1996. Application of new wastewater treatment technologies developed by the Biofocus WT project. WQI Water Quality International Sept./Oct.: 27–30.

Leenen, E. J. T. M., V. A. P. M. Dos Santos, K. C. F. Grolle, J. Tramper & R. H. Wijffels, 1996. Characteristics of and selection criteria for cell immobilization in wastewater treatment. Wat. Res. 30: 2985–2996.

Mobarry, B. K., M. Wagner, V. Urbain, B. E. Rittmann & D. A. Stahl, 1996. Phylogenetic probes for analyzing abundance and spatial organization of nitrifying bacteria. Appl. Environ. Microbiol. 62: 2156–2162.

Murray, R. G. E. & S. W. Watson, 1965. Structure of *Nitrosocystis oceanus* and comparison with *Nitrosomonas* and *Nitrobacter*. J. Bacteriol. 89: 1594–1609.

Oerther, D. B., F. L. de los Reyes & L. Raskin, 1999. Interfacing phylogenetic oligonucleotide probe hybridisation with representation of microbial populations and specific growth rates in mathematical models of activated sludge processes. Wat. Sci. Technol. 39: 11–20.

Østgaard, K., N. Lee & T. Welander, 1994. Nitrification at low temperatures. In Second International Symposium on Environmental Biotechnology. Brighton 4–6 July 1994. Institution of Chemical Engineers, Rugby: 134–137.

Picioreanu, C., M. C. M. van Loosdrecht & J. J. Heijnen, 1997. Modelling the effect of oxygen concentration on nitrite accumulation in a biofilm airlift suspension reactor. Wat. Sci. Technol. 36: 147–156.

Picioreanu, C., M. C. M. van Loosdrecht & J. J. Heijnen, 1998. A new combined differential-discrete cellular automaton approach for biofilm modelling: application for growth in gel beads. Biotechnol. Bioeng. 57: 718–731.

Picioreanu, C., M. C. M. van Loosdrecht & J. J. Heijnen, 1999. Discrete-differential modelling of biofilm structure. Wat. Sci. Technol. 39: 115–122.

Schaechter, M. O., O. Maaloe & N. O. Kjeldgaard, 1958. Dependency on medium and temperature of cell size and chemical composition during balanced growth of *Salmonella typhimurium.* J. Gen. Microbiol. 19: 592–606.

Schramm, A., D. De Beer, H. van den Heuvel, S. Ottengraf & R. Amann, 1998a. *In situ* structure/function studies in waste-water treatment systems. Wat. Sci. Technol. 37: 413–416.

Schramm, A., D. De Beer, M. Wagner & R. Amann, 1998b. Identification and activity *in situ* of *Nitrosospira* and *Nitrospira* spp. as dominant populations in a nitrifying fluidized bed reactor. Appl. Environ. Microbiol. 64: 3480–3485.

Smidsrød, O. & G. Skjåk–Bræk, 1990. Alginate as immobilization matrix for cells. Trends Biotechnol. 3: 71–78.

Stahl, D. A. & R. Amann, 1991. Development and application of nucleic acid probes. In Stackebrandt E. & M. Goodfellow (eds), Sequencing and Hybridization Techniques in Bacterial Systematics. John Wiley & Sons, Chichester: 205–248.

Stahl, D. A., 1997. Molecular approaches for the measurement of density, diversity, and phylogeny. In Hurst, C. J., G. R. Knudsen, M. J. McInerney, L. D. Stetzenbach & M. V. Walter (eds), Manual of Environmental Microbiology. American Society for Microbiology Press, Washington DC: 102–114.

Tanaka, K., T. Sumino, H. Nakamura, T. Ogasawara & H Emori, 1996. Application of nitrification by cells immobilized in polyethylene glycol. In Wijffels R. H., R. M. Buitelaar, C. Bucke & J. Tramper (eds), Immobilized Cells: Basics and Applications. Elsevier Science B. V., Amsterdam: 622–632.

Vogelsang, C. & K. Østgaard, 1996. Stability of alginate gels applied for cell entrapment in open systems. In Wijffels, R. H., R. M. Buitelaar, C. Bucke & J. Tramper (eds), Immobilized Cells: Basics and Applications. Elsevier Science B. V., Amsterdam: 213–219.

Vogelsang, C., A. Husby & K. Østgaard, 1997. Functional stability of temperature-compensated nitrification in domestic wastewater treatment obtained with PVA-SbQ/alginate gel entrapment. Wat. Res. 31: 1659–1664.

Vogelsang, C., K. Gollembiewski & K. Østgaard, 1999. Effect of preservation techniques on the regeneration of gel entrapped nitrifying sludge. Wat. Res. 33: 164–168.

Vogelsang, C., R. H. Wijffels & K. Østgaard, 2000. Rheological properties and mechanical stability of new gel-entrapment systems applied in bioreactors. Biotechnol. Bioeng. 70: 247–253.

Wagner, M., B. Assmus, A. Hartmann, P. Hutzler & R. Amann, 1995. *In situ* analysis of microbial consortia in activated sludge using fluorescently labelled, rRNA-targeted oligonucleotide probes and confocal scanning laser microscopy. J. Microsc. 176: 181–187.

Wagner, M., G. Rath, R. Amann, H.-P. Koops & K.-H. Schleifer, 1995. *In situ* identification of ammonia-oxidizing bacteria. System. Appl. Microbiol. 18: 251–264.

Wagner, M., G. Rath, H.-P. Koops, J. Flood & R. Amann, 1996. *In situ* analysis of nitrifying bacteria in sewage treatment plants. Wat. Sci. Technol. 34: 237–244.

Wagner, M. & R. Amann, 1997. Molecular techniques for determining microbial community structures in activated sludge. In Cloete T. E. & N. Y. O. Muyima (eds), Microbial Community Analysis: The Key to Design of Biological Waste-water Treatment Systems. IAWQ Scientific and Technical Report No. 5, University Press, Cambridge: 61–72.

Watson, S. W., 1971. Reisolation of *Nitrosospira briensis* S. Winogradsky & H. Winogradsky 1933. Arch. Mikrobiol. 75: 179–188.

Watson, S. W. & M. Mandel, 1971. Comparison of the morphology and deoxyribonucleic acid composition of 27 strains of nitrifying bacteria. J. Bacteriol. 107: 563–569.

Wiesmann, U., 1994. Biological nitrogen removal from wastewater. In Fiechter, A. (ed.), Advances in Biochemical Engineering / Biotechnology. Springer-Verlag, Berlin 51: 113–154.

Wijffels, R. H. & J. Tramper, 1995. Nitrification by immobilized cells. Enzyme Microb. Technol. 17: 482–492.

Wijffels R. H., R. M. Buitelaar, C. Bucke & J. Tramper (eds), 1996. Immobilized Cells: Basics and Applications. Elsevier Science Publishers, Amsterdam: 864 pp.